Journal of Natural Sciences Research www.iiste.org
ISSN 2224-3186 (Paper) ISSN 2225-0921 (Online)
Vol.7, No.4, 2017

Geochemical and Geo-thermometers Characteristics of Thermal Groundwater at Khan Ezabeeb Area, in Central Jordan

Abedelkarim Al-Saudi[1] Ibrahim Ahmad Bany Yaseen[2]
1. Ministry of Energy and Minerals Resources, Geology Directorate, Amman, Jordan
2. Institute of Earth and Environmental Sciences, Al-al-Bayt University, Al-Mafraq, Jordan

Abstract
Chemical analysis was conducted of 38 wells discharging thermal fluids in central Jordan near Khan Ezabeeb area. 6 samples of cold water and 7 samples of thermal water were sampled from all over Jordan for comparative analysis; 22 samples and 7 samples were reviewed and studied for stable and radioactive isotope respectively. Chemical characteristics of the thermal fluids were also studied. The data was interpreted by use of WATCH program for speciation and construction of mineral equilibrium diagrams and other graphical representations and classifications. The maximum reservoir temperature for the wells as predicted by calculation of various geo-thermometers exceeds 100°C. There is an evidence of mixing with cold water. The thermal fluids are of bicarbonate type with two main aquifers and the reservoir rocks were mainly marly and cherty limestone. The calculated Quartz and Chalcedony geo-thermometer values for the geothermal well waters indicate reservoir temperature of 60°–80°C' the Na-K-Ca geo-thermometers give mostly higher values; however, calculation of mineral saturation for the geothermal water shows fluid from some wells to be close to the equilibrium at 115°C and some degree of under saturation with anhydrite, fluorite and chalcedony. The chemical composition of the waters in the studied area was governed by water rock interaction in this study the Cl-SO_4-HCO_3, Na- K- Mg triangular diagrams, and stable isotopes were used to classify the geothermal and cold waters and to study some processes in the geothermal system. The geothermal waters are bicarbonate type with some samples of chloride and sulfide - indicating reactions with sedimentary rocks (sandstone). Origins of the fluids are of meteoric water and the age dated between 20,000 years up to 38,000 years.
Keywords: Geochemical, Geo-Thermometers, Thermal Fluids, Age Determination, Khan Ezabeeb, Jordan.

1. Introduction

The geothermal energy is stored between the earth's surface and a specified depth in the crust (Muffler P and Cataldi, 1978). It is measured from local average annual temperature beneath a specified area. The classifying geothermal resources are based on the enthalpy of the geothermal fluids that act as the carrier transporting heat from the deep hot rocks to the surface. Enthalpy, which is considered more or less proportional to the temperature is used to express the heat content of the fluids and helps to estimate their values. Geothermal utilization involves energy production at a rate that may be maintained for a very long time (100–300 years). The production capacity of geothermal systems is quite variable and different systems respond differently to production, depending on their geological setting and nature.

In Jordan, the geothermal waters resources can be related to deep circulation of meteoric water along faults and fractures (Truesdell, 1979; Di Paola G., 1981). The thermal waters can be sub-divided into two groups. The first group includes natural springs in sandstone rock outcrops - these are the main surface manifestation of geothermal energy of Jordan. The second group includes geothermal resources discovered during oil and groundwater explorations within the deep aquifers in the Eastern Jordan deserts and along the Eastern margins of the Dead Sea Rift. The main resources of this group are Shuneh and Makheibeh well fields (Figure 1). The location of all the thermal springs and the hot boreholes dictated to the Dead Sea Rift. Several thermal springs distributed along the Eastern escarpment of the Dead Sea Rift for a distance of approximately 200 km from Mukheibeh thermal field in the North to Afra and Burbeitta thermal fields in the South (Figure 1). Most springs have temperatures below 45°C, except in two localities where the temperatures reach up to 63°C (Zarqa Ma'in and Zara springs). This study focused on the thermal boreholes in Kan Ezabeeb area located within Al Jiza area in central Jordan (Figure 1). The objectives of this study are to analyse the geochemical and geo-thermometer characteristics of the thermal fluids, to assess the maximum reservoir temperatures, the origin of thermal fluids and the heat source and to delineate the evidences of mixing between thermal and cold ground water.

2. Study Area

The Kan Ezabeeb (Kz) thermal water wells are located within Al-Jiza area in the Central part of Jordan about 30 km to the South of Amman at the Palestine grids range from 225,000-285,000E and 85,000-145,000N (Figure 1). The area varies in altitude from a minimum of approximately 680 m above sea level in the western most part of the region, to a maximum of 918 m on Musattarat All Falij in the upper center. The area is along the Wadi Mujib hydrological basin. Many wells drilled in the area - most have water temperatures ranging from 29 to 46^0C. The thermal boreholes are located along the Eastern end of the Zarqa main area along fault zone and close to the

other major fault zones in the area. All boreholes discharge thermal water from two main aquifers, which consist of intercalated limestone. Certain boreholes have the smell of H_2S and some contain iron oxides. Boreholes Kz1-Kz38 have been studied (Figure 1) and sampled for major chemical analysis, to detect traces of metal and some were selected for their stable and radioactive isotope deuterium, ^{18}O, tritium, ^{14}C. Basic field measurements were conducted for the purpose of analysis. The geothermal fluids discharged from the wells in Khan Ezabeeb area are classified as HCO_3 type with pH between 6-8, chloride content from 59 to 433 ppm, and the TDS between 380 to 1,387 ppm. Results of chemical analysis identify two types of aquifers: (1) B2/A7 and (2) Kurnub Sandstone. The chemical composition of fluids from thermal wells indicates that the heat source is in deep circulation and the main flow of the geothermal fluid follows NNE for along the fracture and major faults in the studied area (Saudi A., 1999). The thermal fluids well mixed with cold groundwater in the Central part of the studied area as evident from data for well numbers Kz 1, 6, 19 and 20 as aligned with Cl versus ^{18}O, Br and B models.

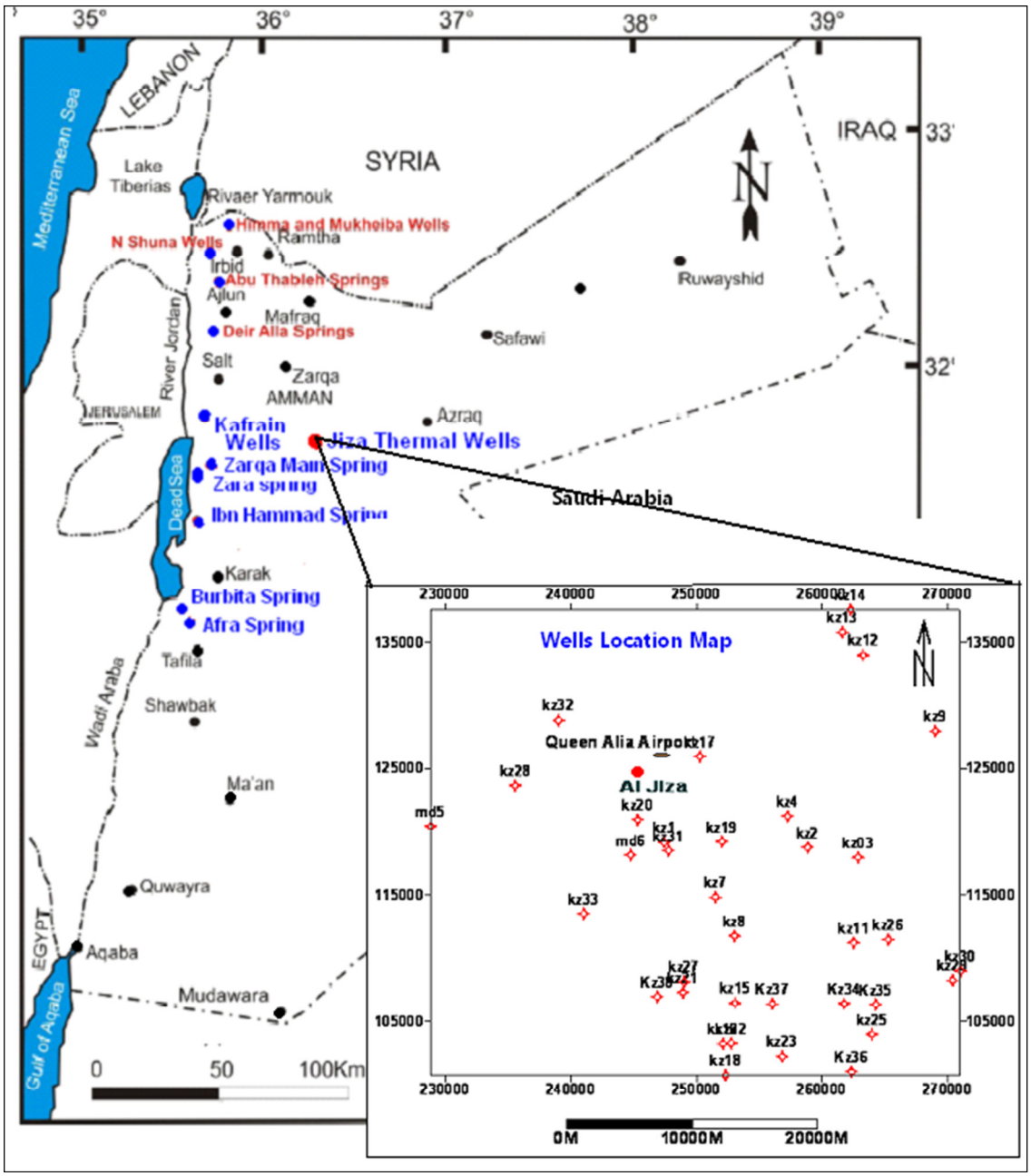

Figure 1: Distribution of geothermal waters in Jordan, and Wells Location Map in the Study Area

3. Geological Setting

The exposed rocks in the area are sedimentary in origin and upper Cretaceous, lower Tertiary and Pleistocene to Recent in age (Jaser D., 1986). The rock sequence is a succession of shallow marine deposits originally lying in

the southern shallow waters of the Tethys Ocean. These consists largely of carbonates that have been moderately tectonically deformed after regression of the Tethys at the close of the Paleocene and later eroded by fluvial processes followed by uplift (Bender, 1974).

The chronological sequence of lithological units shown below. The geological data on this report sourced from the 1.50.000, geological map of (Jaser D., 1986). The formation covers of the study area listed in Table 1. The Amman silicified limestone formation appears like several small outcrops in the mountainous Central area. The uppermost part (15-23 m) exposed in the area consists of thin to thick bedded chert, with grey limestone of micritic and wackestone texture with a thin bed of yellowish marl on the top.

Table 1: Chronological and lithological sequence of the study area.

Formation	Stage	Period
Alluvial and Wadi gravel	Holocene	Quaternary
Urn Rijam chert limestone	Eocene	Quaternary
Muwaqqar chalk marl	Paleocene	Tertiary
Al Hisa posphorite	Mastrichtain	Upper Cretaceous
Amman silicified limestone	Campanian	Upper Cretaceous

The formation was probably deposited in a transgressed sea. Chalks and marls were deposited in deeper waters and the deposition of chert-limestone occurred towards the shore (Futyan, 1968). The AL Hisa Phosphorite Formation mostly consists of silicified phosphorite - phosphorite bearing oyster and phosphate layers. Chert is less as compared to the Amman formation, where there is a distinct increase in the proportion of limestone and phosphate. Phosphate is economically important in Jordan. However, the phosphate bed in this area does not exceed 50 cm and occurs in the upper part of the formations. Soft pelloids and granules in the phosphatic chert as well as the underlying phosphatic limestone within the formation vary in texture from micrite interbedded with phosphate to chalky marl. The thickness of this formation ranges from 25-50 m. The Muwaquar chalk-marl formation consists of white chalk, chalky marl, chalky limestone, rnicritic limestone and chert. The upper part interbedded with dark grey to brownish chert and the lower part consists of thick beds of white to light grey cherts; white chalk with light grey layers and large limestone concretions reach up to 2 m diameter in certain places. The thickness of the entire formation is approximtely70 m and the age is in the range of Maestrichtian-Danian-lower Paleocene. The Um Rijam chert limestone formation consists of pale yellow to light red chalk marl and chalky limestone with layers of light grey-to-grey chert in the form of lenses. The thickness of this formation is approximately 80 m and the age of the chert limestone is considered upper in range of Paleocene-lower Eocene (Bender, 1974). Alluvial and Wadi gravel represent the detrital materials of this sediment ranges from coarse-grained and gravel of ill sorted sub-angular to rounded pebbles; the age ranges from Holocene to recent sediments.

The Structural geology of the study area shows that two dominant fault trends within the area are NW-SE and E-W. The Zarqa main fault set is an E-W group of faults and linear features occur in the central western part of the map area. The Wadi Al-Hammam and the Masattarat AL Falij fault sets represent the major NW-SE trend, and have given rise to the uplifted plateau of the Umm Rijam formation. The folding in the map area is of three types:gentle folding associated with regional compression, folding occurring adjacent to faults and directly associated with drag during faulting and folding in interference structures caused by the interaction of E-W and NW-SE faulting influences.

4. Sampling and Analytical Techniques

Thirty-seven thermal well water samples collected from the surrounding areas of Khan Ezabeeb within Dead Sea Basin. Five cold water well and four thermal well samples collected outside of the study area **(**Figure 1). Two type water samples collected by 1-Liter polyethylene bottles; first sample original and second has added 1.5ml of 1N HNO_3. Forten thermal water samples collected used to analysis of stable isotope composition for δ18O and δD. Seven thermal water samples collected used to analysis of Age determination for C^{14}. The chemical analyses of the samples determine in water authority lab (Laboratories and Quality Affairs) for Na, K, Mg, Ca, Cl, SO_4, NO_3, SiO_2, CO_2, Li, NH_4, Fe, Mn, Cu, Pb, Zn, Al, F, Br, B, As, Sr by using Ion Chromatography analysis for Ca, Mg, K, Na. Br, Cl, SO_4 and NH4. Inductively Coupled Plazma (ICP) and Atomic Emission Spectroscopy (AAS) analysis for Li, Fe, Mn, Cu, Pb, Zn, Al, B, As, Sr. Molybdosilicate for analysis of SiO_2. $\delta^{18}O$ analysis by CO_2 Equilibrium/Delta Plus XP/IRMS HDO using Platinum Catalyst Deuterium (δD) analysis by Delta Plus XP/IRMS HDO/Mass Spectrometry using Platinum Catalyst analysis .C^{14} Measurement by Benzene Synthesis Line and Liquid Scintillation Counter. The ^{34}S sulphates analysis in Pakistan atomic energy agency. The H_2S, HCO_3 were titration in the field. The Total Dissolved Solids (TDS) measured by Instrumental measurement, PH by PH-meter, Electrical Conductivity (EC) by Conductivity meter in the field. The result listed in Table (2, 3, 4).

5. Results

5.1. Geochemical characteristics of thermal fluids

The composition of thermal fluids depends on many factors. The most important is temperature dependent reactions between host rock and fluid. Leaching also plays an important role when the amount of a particular constituent is too small to achieve equilibrium or does not participate in any temperature dependent minerals/solute equilibrium. Processes such as mixing, boiling and cooling may also have significant influence on the final composition of the geothermal water. Chemical analysis was conducted for the samples for boreholes Kz1-038 in Central Jordan (Figure 1) for elements and compounds such as $\delta^{18}O$, δD, Na, K, Mg, Ca, Cl, HCO_3, SO_4, NO_3, SiO_2, H_2S, CO_2, Li, NH_4, Fe, Mn, Cu, Pb, Zn, Al, F, Br, B, Sr. In addition, field measurements were done for T°, pH ,TDS and EC. Fieldwork was conducted in two seasons - summer and winter in order to monitor the temperature and any changes in chemical composition of these boreholes on a monthly basis. The analysis indicates that there is no significant change (> 1° C) in temperature further, re sampling 15 wells shows any changes in chemical composition. All the samples were analysed at the Water Authority Laboratories having a national government qualification for analysis of all types of water samples.

Results of the chemical analysis from the 38 wells are listed (Table 2**)**. For comparison, the results of chemical analysis from different locations for cold water (Table 3), and chemical analysis for chosen thermal water from hot spring from different site of Jordan (Table 4) have been listed. The WATCH program for speciation and calculation of mineral equilibrium was used to process the data from the wells. The data was plotted in different triangular classification diagrams, mixing model diagrams, and for comparative analysis between chloride content and other components. Fourteen wells were selected for the plotting of mineral saturation log (Q/K) diagrams.

5.2 Fluids Classification

5.2.1Schoeller Diagram

This diagram used to classify the type of waters. It may be used to map the changes over a period for different types of waters that have been plotted. The log concentrations of fluid constituents from numerous analyses can be connected with a line since use of logarithmic values provides wide range of concentrations. The effect of mixing with dilute water (as well as gain or loss of steam) is to move the connecting line vertically without changing its shape (Truesdell, 1991). Different water types could be displayed by crossing lines. In **(**Figure 2a**)** a Schoeller diagram for water from 38 wells clearly shows bicarbonate waters and indicates mixing between thermal and cold groundwater. Data also indicates that thermal water has slight presence of sulfate and higher calcium and chlorine content. The diagram proves that there is some mixing with cold waters from the field or the neighboring area.

The Schoeller diagram is prepared according to the percentage of the ions as mill equivalent value. Schoeller diagram for the selected cold-water samples (Figure 2b)**,** shows a slight range in logarithmic values of potassium and represents two types of waters - bicarbonate and sulfate rich water which represent the Rahma well in the area close to Rift valley in Wadi Araba.

Table 2: Chemical analysis of thermal water wells study.

Well Samples No.	Kz1	Kz2	Kz3	KZ4	MD5	kz6	Kz7	Kz8	Kz9	Kz10	Kz11	Kz12
Na mg/l	36.6	72.9	112.2	83.0	64.1	43.0	121.0	213.1	51.8	57.0	245.0	44.0
K mg/l	2.0	3.1	4.7	3.1	15.2	2.0	7.1	10.6	2.3	4.0	8.2	2.0
Mg mg/l	34.8	54.6	49.6	51.3	52.9	30.0	66.0	99.8	31.3	37.0	133.0	27.0
Ca mg/l	94.2	110.0	105.6	123.2	76.6	100.0	159.0	211.2	60.3	80.0	223.0	64.0
Cl mg/l	59.2	158.1	178.7	204.9	164.1	71.0	208.0	402.4	101.9	99.0	424.0	87.0
HCO3 mg/l	397.7	418.5	337.9	385.5	269.6	365.0	445.0	464.8	218.4	227.0	432.0	250.0
SO_4 mg/l	51.8	100.8	177.1	103.2	119.0	50.0	289.0	450.7	62.4	146.0	570.0	41.0
NO_3 mg/l	4.49	0.4	0.5	0.4	0.5	3.3	0.3	0.4	2.69	0.2	1	0.3
SiO_2 mg/l	13.8	17.6	21.8	16.7	19.4	9.7	11.1	19.9	19	19.4	11.2	22.4
H_2S	0.1		0.93		0.1	0.1		0.3	0.27	1.70		0.29
CO_2	90.0		175.0		46.0	30.7		230.0	17.5	33.3		20.0
Li mg/l	0.01	0.014	0.02	0.012	0.032	<0.01	0.02	0.033	0.011	0	0.03	0
NH4 mg/l	0.12	0.14	0.26	<0.1	0.49	<0.01	<0.01	<0.1	0.22	0.1	0.63	0.2
Fe mg/l	<0.01	<0.01	<0.01	<0.01	0.05	< 0.02	<0.02	<0.01	0.08	0.1	1.34	0.2
Mn mg/l	<0.01	0.04	<0.01	<0.01	<0.01	< 0.01	<0.01	<0.01	0.01	0.1	0.02	0
Cu mg/l	<0.01	<0.01	<0.01	<0.01	<0.01	<0.01	<0.01	<0.01	<0.01	0	<0.01	0
Pb mg/l	<0.01	<0.01	<0.01	<0.01	<0.01	< 0.01	<0.01	<0.01	<0.01	0	<0.01	0
Zn mg/l	<0.01	<0.01	<0.01	<0.01	<0.01	0.1	0.13	<0.01	<0.01	0	<0.01	0.3
Al mg/l	<0.01	<0.01	<0.01	<0.01	0.04	0	<0.01	<0.01	0.01	0	<0.01	0
F mg/l	0.46	1.1	1.34	1	1.7	0.6	1.62	1.03	2.04	1.9	1.29	1.5
Br mg/l	<0.05	0.71	0.84	0.96	0.88	< 0.05	0.85	1.71	0.55	0.5	<0.05	0.5
B mg/l	0.11	0.17	0.34	0.21	0.23	0.2	0.53	0.93	0.015	0	0.9	0
As mg/l	<0.01	<0.01	<0.01	<0.01	<0.01		<0.01	<0.01	<0.01		<0.01	
Sr mg/l	-	-	-	-	-	0.9	3.3	-	2.27	2.9	5.9	2.0
Na mg/l	41.0	38.0	238.0	102.6	71.3	86.7	42.6	79.4	37.5	198.0	174.0	174.0
K mg/l	2.0	2.0	8.0	7.8	2.7	3.1	2.0	5.1	2.0	7.0	7.0	5.9
Mg mg/l	29.0	31.0	80.0	54.6	40.7	58.4	30.3	56.1	30.8	69.9	79.4	65.3
Ca mg/l	70.0	60.0	177.0	219.8	124	133	100.0	140.0	79.4	145.0	187.0	171.0
Cl mg/l	75.0	69.0	376.0	344.4	120	151	70.6	124.0	59.2	433.0	263.0	254.0
HCO_3 mg/l	273.0	250.0	396.0	419.7	469	506	365.0	479.0	312.0	307.0	476.0	420.0
SO_4 mg/l	54.0	51.0	431.0	419	84.5	121	50.1	190.0	55.7	225.0	433.0	386.0
NO_3 mg/l	0.3	3	0.5	0.32	3	0.2	3.3	0.6	4.9	0.8	0.8	0.6
SiO_2 mg/l	18.3	18.8	19.7	16.6	14	15.1	9.7	11.0	9.5	12.3	11.2	10.6
H_2S						0.08				1.6	1.0	
CO_2						210.0	263.3	345.5	225.0	73.4	240.0	303.0
Li mg/l	0	0	0	0.029	0.01	0.01	<0.01	0.02	<0.01	0.03	0.03	0.03
NH_4 mg/l	0.2	0.2	0.6	0.263	<0.1	<0.1	<0.01	<0.01	<0.01	0.34	0.23	0.17
Fe mg/l	0.1	0.1	2.1	1.43	8.8	0.04	<0.02	0.65	<0.02	0.12	0.94	5.1
Mn mg/l	0	0	0	0.09	0.12	<0.01	<0.01	<0.01	<0.01	0.05	0.01	0.07
Cu mg/l	0	0	0	<0.01	<0.01	<0.01	<0.01	4.33	<0.01	<0.01	0.01	0.015
Pb mg/l	0	0	0	0.012	<0.01	<0.01	<0.01	0.24	<0.01	<0.01	0.02	<0.01
Zn mg/l	0	0	0	<0.01	<0.01	0.03	0.07	X	0.04	<0.01	0.07	0.12
Al mg/l	0	0	0	0.21	<0.01	<0.01	0.02	<0.01	<0.01	0.02	0.02	0.01
F mg/l	1.4	1.4	1.4	1.24	1.26	1.48	0.61	1.49	0.5	1.48	1.16	1.21
Br mg/l	0.3	0.4	1.6	1.28	0.69	0.77	<0.05	0.58	0.44	<0.05	<0.05	<0.05
B mg/l	0	0.9	0.9	0.53	0.1	0.04	0.24	0.27	0.12	1.53	0.97	0.88
As mg/l	-	-	-	<0.01	<0.01	<0.01	<0.01	<0.01	<0.01	<0.01	<0.01	<0.01
Sr mg/l	2.2	2.0	4.6	3.91	2.5	2.2	0.93	3.3	0.83	5	4.83	3.9

Table 2 Continued

Well Samples No	Kz 24	Kz 25	Kz 26	Kz 27	Kz 28	Kz 29	Kz 30	Kz 32	Kz 34	Kz 35	Kz 36	Kz 37	Kz 38
Na mg/l	148	134	170	174.8	42.0	153.0	154.0	41	190	187	125	207	161
K mg/l	7	5.1	5.5	6.6	2.0	7.0	8.0	5	7	9	4	8	8
Mg mg/l	69.3	49.9	78.1	60.1	35.0	62.0	58.0	25	66	70	42	69	60
Ca mg/l	194	140	204	137.5	113.0	158.0	141.0	71	182	174	110	182	145
Cl mg/l	217	172	267	372	64.0	225.0	226.0	65	250	259	174	338	330
HCO_3 mg/l	465	431	488	305	423.0	420.0	406.0		459	445	293	401	372
SO_4 mg/l	399	246	422	197.8	66.0	312.0	263.0	51	411	385	240	387	387
NO_3 mg/l	6	0.3	0.5	0.6	5.5	0.5	0.5	13.7	<0.01	<0.1	<0.1	<0.1	0.4
SiO_2 mg/l	15.1	13	13.9	-	13.0	20.2	20.5	11.6	17	14.2	17.4	17.7	16
H_2S		0.07		2.1				0.1			0.5	0.23	0.09
CO_2	335.4	237.0	352.0	154.0				30.8			99.5	187.0	114.0
Li mg/l	0.02	0.02	0.02	-	< 0.01	0.023	0.022	<0.01	0.02	0.02	0.01	0.02	0.02
NH_4 mg/l	0.15	0.2	0.13	-	0.03	0.7	0.554	<0.02	0.06	0.07	0.12	0.26	0.51
Fe mg/l	0.12	0.17	1.44	0.64	0.08	0.06	1.34	0.03	0.01	0.68	0.37	0.05	0.01
Mn mg/l	0.018	0.04	0.027	0.016	<0.01	<0.01	0.02	<0.01	<0.01	0.03	<0.01	<0.01	<0.01
Cu mg/l	<0.01	<0.01	<0.01	<0.01	< 0.01	<0.01	<0.01	<0.01	<0.01	<0.01	<0.01	<0.01	<0.01
Pb mg/l	<0.01	<0.01	<0.01	0.01	<0.01	<0.01	<0.01	<0.01	<0.01	<0.01	<0.01	<0.01	<0.01
Zn mg/l	<0.01	<0.01	0.07	0.014	0.08	<0.01	0.06	<0.01	0.04	0.02	<0.01	<0.01	<0.01
Al mg/l	0.05	<0.01	0.02	-	<0.01	0.06	0.05	0.04	<0.01	<0.01	<0.01	<0.01	<0.01
F mg/l	1.24	1.15	1.01	-	0.75	1.54	1.43	0.8	0.99	1.23	1.12	1.07	1.28
Br mg/l	1.54	0.94	2.74	-	0.78	0.74	0.77	0.31	0.81	0.99	0.53	1.43	1.51
B mg/l	0.21	0.2	0.36	-		0.5	0.44						
As mg/l	<0.01	<0.01	<0.01	-									
Sr mg/l	4.2	2.8	4.3	-	0.9	3.87	3.65	1.21	3.05	2.9	2.1	3.6	3.2

Table 3 Chemical analysis of the cold water well for the outside of the study area.

Well Samples No	Shoubak1	Shoubak2	Rahma	Dana	Rawath
Na mg/l	54.3	26.5	168.4	20	14.5
K mg/l	8.2	1.2	6.6	7.4	0.4
Mg mg/l	32.6	33.7	25.4	28.2	18.6
Ca mg/l	108.4	52.5	45.7	83.8	61.3
Cl mg/l	95.1	44.4	179.3	49.3	42.2
HCO_3 mg/l	356.24	257.42	162.26	322.08	176.9
SO_4 mg/l	73.9	32.2	198.7	29.8	18.7
NO_3 mg/l	34.7	19.65	12.97	16.81	37.99
SiO_2 mg/l	20	14.2	21.3	21.7	12.3
Fe mg/l	0.12	0.02	0.1	0.05	0.34
Al mg/l	0	0	0.025	0.025	0.13
F mg/l	0.68	0.38	2.27	0.38	0.27
Br mg/l	0.38	0	0.3	0	0.46
B mg/l	0.15	0.08	0.36	0.04	0.03
Sr mg/l	0.8	0.35	0.92	0..36	0.38

Table 4 Chemical analysis of the thermal well fluid outside the study area

Well Samples and spring No.	SH1	HM1	HM2	Afra spring
Na mg/l	84.9	41.4	117	35.40
K mg/l	5.9	3.1	15.3	2.00
Mg mg/l	50.1	45	35.1	18.40
Ca mg/l	80.2	85	124	47.90
Cl mg/l	125	56.8	205	60.00
HCO_3 mg/l	404	414	293	
SO_4 mg/l	79.7	60	183	56.20
NO_3 mg/l	2.8	0.41	0.78	<0.1
SiO_2 mg/l	20.7	17.2	28.1	21.50
CO_2	291.4	298.6	211.3	
Li mg/l	0.023	<0.01	0.1	0.02
NH4 mg/l	0.44	0.27	1.79	<0.02
Fe mg/l	0.05	0.05	0.3	0.22
Mn mg/l	<0.01	0.05	0.22	0.06
Cu mg/l	<0.01	<0.01	<0.01	
Pb mg/l	<0.01	<0.01	<0.01	
Zn mg/l	<0.01	<0.01	0.05	<0.01
Al mg/l	0.01	<0.01	0.03	<0.01
F mg/l	0.71	0.61	1.41	0.43
Br mg/l	0.2	<0.05	2.2	0.17
B mg/l	0.05	0	0.06	
As mg/l	<0.01	<0.01	<0.01	
Sr mg/l	1.3	1.07	4.3	0.46

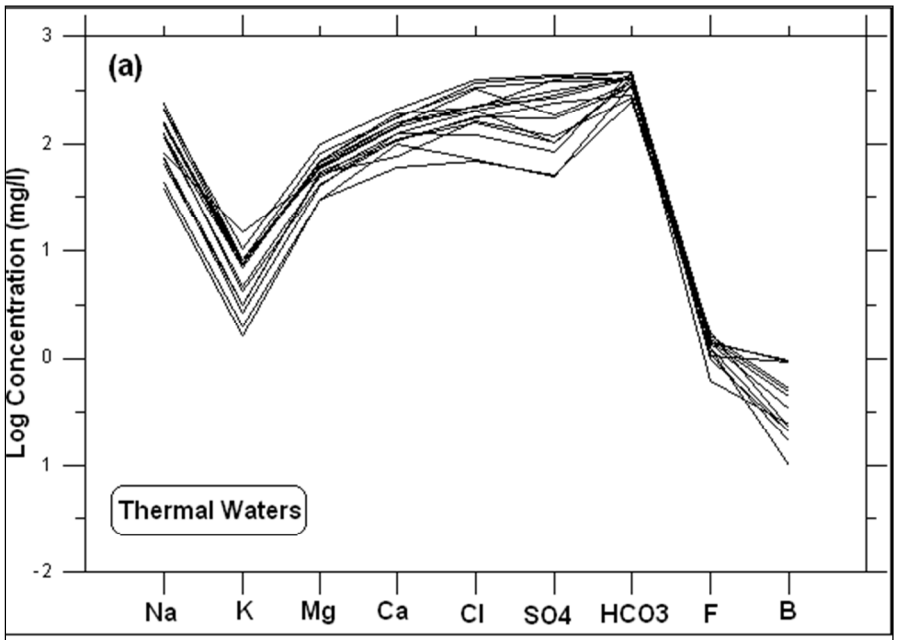

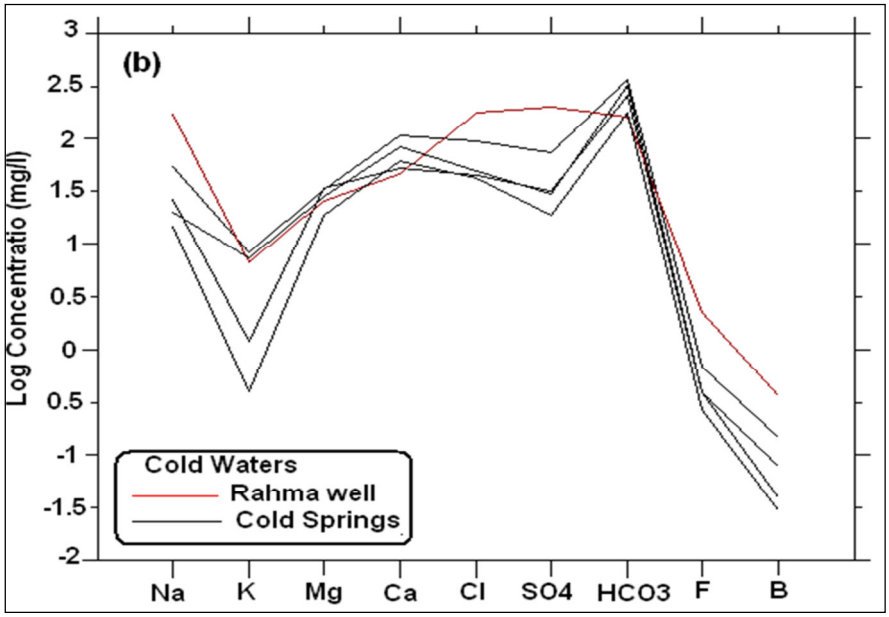

Figure 2: (a) Schoeller Diagram for Thermal Water Wells, (b) Schoeller Diagram for Cold Water Wells.

5.2.2. Cl-SO_4-HCO_3 Triangular diagram

The classification of thermal waters a triangular diagram Cl-SO_4-HCO_3 was used for the classification of natural waters. Giggenbach (1991) described this diagram for the classification of geothermal water. It helps to discern immature, unstable waters and may give an initial indication of mixing relationships or geographic groupings. The diagram resembles the popular diagram proposed for the classification of natural waters. It may give a preliminary statistical evaluation of groupings and trends. The degree of separation between data points for high chloride and bicarbonate waters provides an estimate of the relative degrees of interaction of the CO_2 changed fluids at lower temperature and at the HCO_3 contents increasing with time and distance traveled underground.

The results of calculations and plotting of analytical samples from Central Jordan shown in (Figure 3). Most samples plotted in the high bicarbonate region or mixed groundwater. The low temperature waters and four other samples are in vicinity of the field of chloride and sulfate waters, which probably due to the gypsum and anhydrite content but are still within the bicarbonate water range. This suggests some degree of mixing. Only two sample plots were in the chloride field.

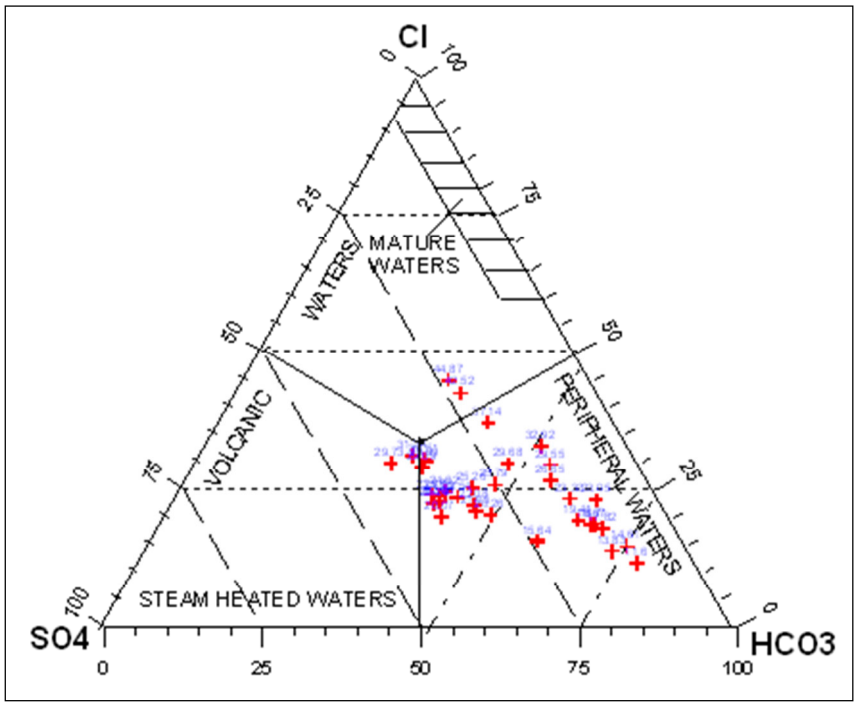

Figure 3: The Cl-SO_4-HCO_3 Triangular Diagram for Thermal Waters Samples from Khan Zabeeb area.

5.2.3 Na-K-Mg Triangular diagram

Giggenbach, (1988) constructed the Na-K-Mg diagram based on the temperature dependence of the two reactions:

K-Feldspar + Na^+=Na-Feldspar + K^+

2.8K-Feldspar + 1.6Water + Mg^{2+} = 0.8Mica + 0.2Chlorite + 5.4Silica+2K^+

The diagram is used to evaluate equilibrium conditions between the geothermal water and reservoir rocks. The main advantage of this diagram is its ability to graphically represent the position of a large number of samples simultaneously, permitting delineation of mixing trends and groupings. It separates well the position of waters resulting from the two end member processes, rock dissolution and equilibration. The Figure 4, depicts all the samples plotted in the area of immature waters very close to the Mg corner of the diagram, indicating that the thermal fluids area has a mixture of cold groundwater. The relatively high Mg concentration is due to the bicarbonate type of the water. Therefore, it is not possible to use K-Na and K-Mg geo-thermometers to estimate reservoir and discharge temperatures for the thermal fluids.

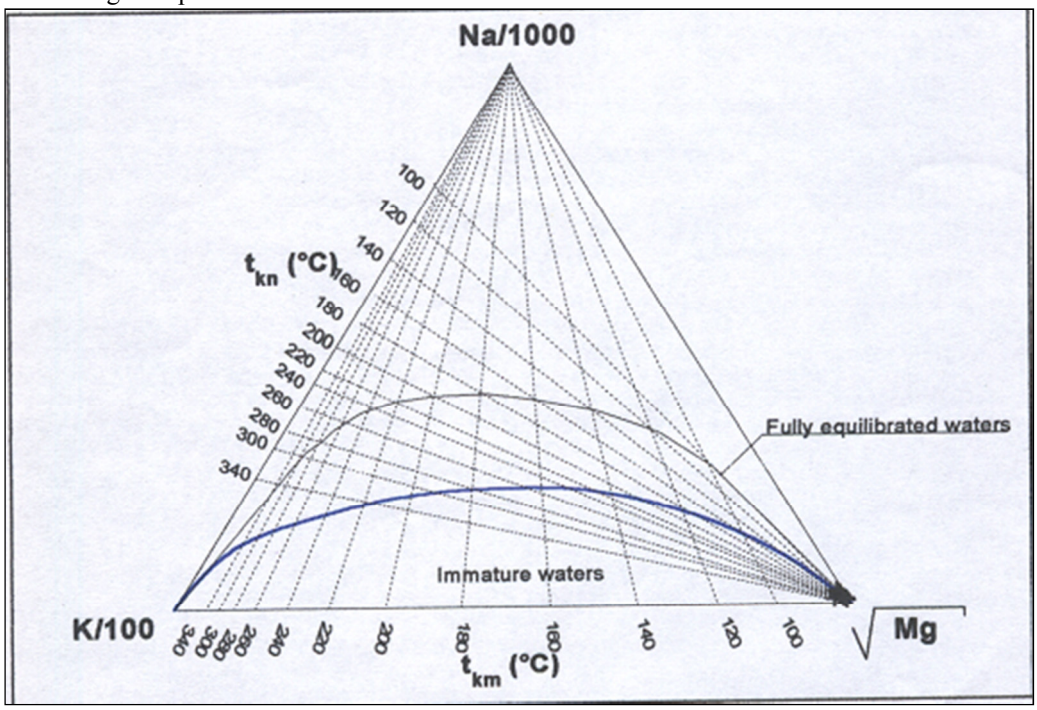

Figure 4: The Na- K- Mg Triangular Diagram for the Thermal Waters from Khan Zabeeb area.

5.3. Origin of Geothermal Waters

5.3.1 Stable Isotope Composition

Graig, (1961) studied the stable isotope of the hydrogen and oxygen in natural waters. When water evaporates in a system where thermodynamic equilibrium is maintained, the concentration of the components in the vapor and liquid phases are controlled by the respective vapor pressure. Experimental studies have shown that the isotope relationship in meteoric water is governed by the natural water cycle of evaporation–condensation. Under equilibrium conditions, the oceanic precipitation is progressively depleted in the heavy isotopes as a function of distance of the precipitation from the local atmospheric reservoir . Two facts are observed - first that there would be an approximate constant ratio of $\delta D/\delta^{18}O$ indicating depletion relative to a given standard. Therefore, water derived from the meteorological cycle has a natural label and can be distinguished from any water derived from a source with a different isotopic relationship (Clark and Fritz, 1998). This may provide a method of detecting juvenile components. Second, that there is a general decrease in the heavy isotopic concentration as the latitude varies from equator to the poles; this reflects a continuous loss of vapor from the air masses moving towards the poles. Consequently, precipitation has a latitude effect which is often complex and depends on local metrological conditions. Hence, there are substantial time variations in the heavy isotopic concentration of local precipitation. The fact that precipitation is labeled by its isotopic concentration suggests an application along two lines - first, the ratio $\delta D/\delta^{18}O$ in thermal water indicates any admixtures with components that are not derived from oceanic meteorological systems and second, thermal fluid and ground water in general may percolate a long distance underground. Their isotopic concentration may differ from that of local precipitation at the springs; hence, a systematic study of the precipitation in the region may lead to the detection of a recharge area. This method is applicable both to groundwater hydrology and to geothermal work. When oxygen isotopes are

exchanged between hot rock and the circulating water, it is called oxygen shift. The extent of the oxygen isotope shift depends on the interaction temperature, water rock ratio, interaction time and permeability of the rock. Generally, low temperature and high water – rock ratio and low interaction time result in a low oxygen isotope shift. Oxygen shift may also be due to the presence of "andesite water" (Giggenbach, 1991**).**

Refer Figure 5**,** isotopic data differentiates between the three possible types of origin of thermal water i.e. magmatic, oceanic and meteoric. Ranges of ^{18}O and ^{2}H of all the samples are -6.74 to -5.06‰ and –34.90 to –24.85‰ respectively (Table 5). These data shows no presence of any significant amount of magmatic water which generally has (^{18}O: +6 to +9‰ and (^{2}H: -40 to -80‰) (Pearson J. and Rightmire T., 1980; Giggenbach, 1992). The possibility of oceanic origin of these waters is ruled out because their (^{18}O and ^{2}H are approximately 0‰). Therefore, the origin of these waters is obviously meteoric. In (^{18}O vs. ^{2}H diagram, the samples (except two outliners) make a trend line of equation: (^{2}H = 5.7 (^{18}O + 3.8). The slope indicates dominance of evaporation/steam separation process. Location of all the data points below the LMWL (^{2}H = 8 ^{18}O + 25) also confirms the evaporation process. The Figure 5 includes samples from well numbers 8, 11, 16, 22, 25, 26, 29, 30 with highly depleted levels, indicating that the precipitation took place in high mountains to the Eastern parts at Jabal El-Mudaisesat mountain. Other samples from well numbers 6, 13, 19 show characteristics with enriched samples indicating low attitudes and precipitation in the Western Madaba Mountains.

In a geothermal system, ^{34}S of sulphates with a magmatic origin ranges between 0‰ and +2‰ CDT (Canyon Diablo Troilite) and sulphates resulting from the dissolution of evaporates can have ^{34}S ranging from +10 to +35‰ whereas in modern oceanic sulphates its value is about +20‰ (Krouse, 1980). The ^{34}S values of sulphates of hot springs are in the range of 6.56 to 10.81‰. It shows that the sulphates are neither of magmatic origin nor of modern oceanic origin. Relatively low values of ^{34}S indicate the major contribution of sulphates derived from reduced sulphur compounds such as sulphide minerals and/or organic sulphides (Pearson Jr. and Rightmire T., 1980**)**.

Table 5: Stable isotope composition $\delta^{18}O$ and δD of the wells study

Well samples No.			Well samples No.		
KZ1	-5.56	-26.3	KZ20	-5.07	-24.8
KZ2	-6.60	-32.1	KZ21	-6.24	-32.1
KZ3	-6.07	-31.4	KZ22	-6.44	-33.4
KZ4	-6.40	-32.0	KZ23	-6.59	-33.5
MD5	-5.61	-27.4	KZ24	-6.74	-34.1
MD6	-5.06	-25.3	KZ25	-6.71	-34.6
KZ7	-5.67	-29.7	KZ26	-6.63	-34.2
KZ8	-6.33	-32.8	L za	-4.84	-35
KZ9	-5.95	-31.0	zq	-3.73	-28.8
KZ11	-6.44	-34.3	Kz31	-5.35	-26.2
KZ 16	-6.60	-32.7	Kz32	-5.3	-26.2
KZ17	-6.05	-32.1	kz10	-6.3	-32.9
KZ18	-6.03	-31.0	kz30	-6.41	-34.9
KZ19	-5.37	-27.8			
MD : Madab wells Zq: Zarqa Main KZ**:** Khan Ezabeeb					

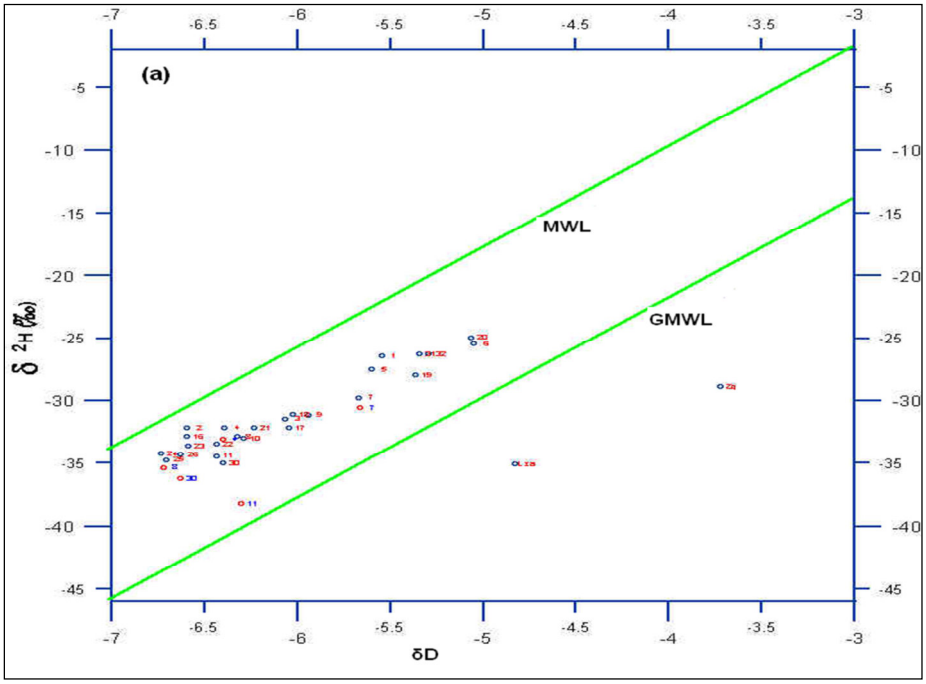

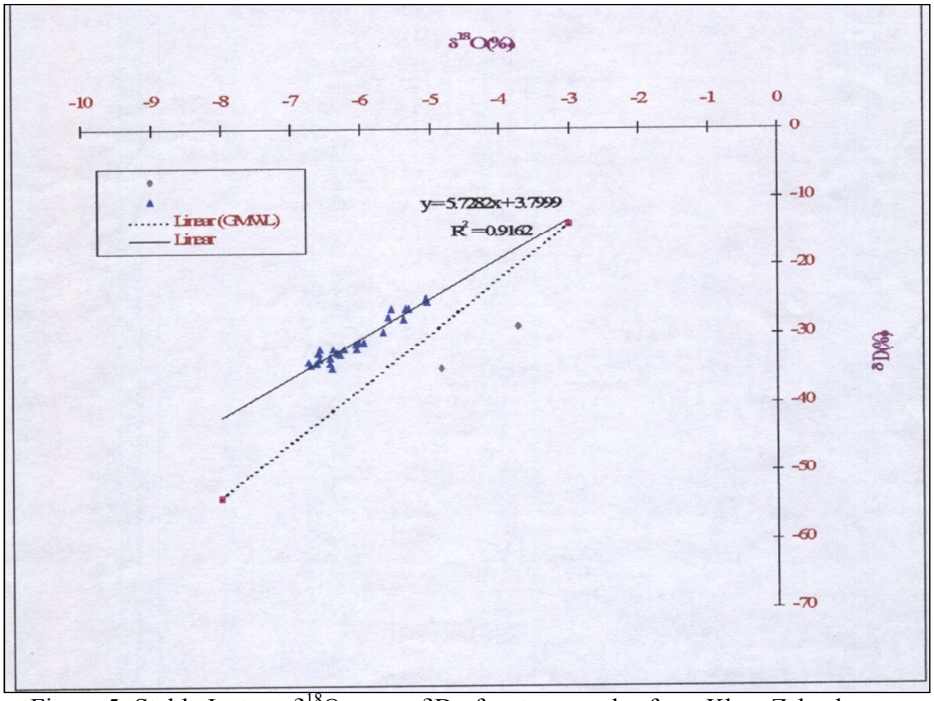

Figure 5: Stable Isotope $\delta^{18}O$ verses δD of water samples from Khan Zabeeb area

5.4 Age of the Thermal Waters

5.4.1. Carbon-14 (^{14}C) Dating

The radioactive ^{14}C is used to determine the age of groundwater. The method can date carbon-containing material from the last 50,000-60,000 years. In general, carbon in groundwater can be derived from various sources such as atmospheric, soil and organic origin, leached from rocks and from magmatic sources in volcanic areas (Pearson et. al., 1970). Generally, age based on the ^{14}C method shows time since groundwater gets isolated from the atmosphere and the soil zone.

Radiocarbon dating based on measuring the loss of the parent radionuclide (^{14}C) in a given sample. This represented by the decay equation:

$$a_t = a_0 . e^{-\lambda t} \quad (1)$$

Where $\mathbf{a_0}$ is the initial activity of the parent nuclide, and 'a_t' is its activity after some time, t. The decay constant λ is equal to $In2/t_{1/2}$. For ^{14}C, $t_{1/2}$ is 5730 years, and this equation simplifies to:

$$t = -8267 \ . \ln \left[\frac{a_t {}^{14}C}{a_0 {}^{14}C} \right] \quad (2)$$

As simple radioactive decay is rare, dilution and loss by geochemical reactions both within the soil and along the flow path must be addressed first. The most typical reactions include dissolution of calcite/dolomite, exchange with the aquifer matrix, oxidation of "old" organic matter found within the aquifer and other biochemical reactions.

The dilution of ^{14}C through reaction is accounted for in the decay equation by the dilution factor or fraction q and the above equation is further modified to:

$$t = -8267 . \ln \left[\frac{a_t {}^{14}C}{q . a_0 {}^{14}C} \right] \quad (3)$$

For dating with the available data, $\delta^{13}C$ mixing model can provide an approximate measure of ^{14}C dilution by carbonate dissolution. The $\delta^{13}C$ mixing model allows for incorporation of ^{14}C-active DIC during carbonate dissolution under open system conditions, and subsequent ^{14}C dilution under closed system conditions. Clark and Fritz, 1998; Pearson 1965; Pearson and Hanshaw 1970 first introduced a $\delta^{13}C$ correction based on variations in ^{13}C abundance.

$$q = \frac{\delta^{13} C_{DIC} - \delta^{13} C_{carb}}{\delta^{13} C_{soil} - \delta^{13} C_{carb}} \quad (4)$$

where:

$\delta^{13}C_{DIC}$ = measured ^{13}C in groundwater

$\delta^{13}C_{soil}$ = $\delta^{13}C$ of the soil CO_2 (usually close to -23‰)

$\delta^{13}C_{carb}$ = $\delta^{13}C$ of the calcite being dissolved (usually close to 0‰)

$\delta^{13}C$ of soil CO_2 was determined in the possible recharge area and other parameters are taken as generally found in literature e.g. pH: 6.5, original ^{14}C activity: 100 pmc, partial pressure of soil CO_2: 0.007, $\delta^{13}C$ of carbonate: 0‰.

Any process that adds removes or exchanges carbon from the DIC pool and thereby alters the ^{14}C concentrations affects the ^{13}C concentrations. In such cases, ^{14}C activity is very low and $\delta^{13}C$ is quite depleted. Such values are also found when CO_2 derived from decomposition of very old organic matter is dissolved in water. If this process occurs, the $\delta^{13}C$ mixing model gives erroneous results. Obtaining the q-factor by carbon isotope mass balance (Eq. 4), ages were estimated as shown in the (Table 6**)**.

Ground water age must increase along a flow path, the age of mixed water has to increase along a flow path; thus the mixture should be older than the youngest mixing water. Seven samples were analysed for ^{14}C (Table 6). The data shows that the age of the thermal fluids ranges between 20,000-37,000 years. The age from the fluid from well number 31 is 20,000 and well numbers 27 and 22 is 30,000 years. These indicate an increasing age of the thermal water from North to South. This is in alignment with the other models that suggest that the mixing of thermal fluids take place in the Northern and Central parts of the fields and a general flow direction is from North to South.

Table 6: Age Determination of the thermal water wells study samples.

well samples No	^{14}C(PMC)	^{13}C (™)(‰)	Dilution factor (q)	Age (years)
MD5	0.79	-4.89	0.212	27219
Kz9	2.91	-9.42	.409	21860
Kz10	1.48	-8.58	.373	26678
Kz22	1.75	-15.57	.677	30219
Kz27	1.24	-11.36	.494	30461
Kz30	.67	-14.8	.643	37737
Kz31	4.83	-13.52	.588	20659

5. 5. Geo-thermometers

One of the most applied methods in the investigations of geothermal resources involves prediction of sub-surface

temperature using chemical geo-thermometers. It is useful to determine the main up flow zones in a geothermal system and the sub-surface temperatures of reservoirs. Cooling of the water may occur by conduction, boiling and/or mixing with cold water, and comparison of different geo-thermometers may be helpful to interpret those processes. The temperatures in geothermal reservoirs are generally not homogeneous but variable both horizontally and vertically; so geo-thermometry is useful for revealing the temperature of the aquifer feeding the drill holes. Temperatures encountered in a deep drill hole may be higher than those indicated by chemical geo-thermometry particularly if the waters investigated are fed by shallow aquifers (Arnoórsson, 1991).

5.5.1. Silica Geo-thermometers

The solubility of all silica minerals decreases drastically as temperature decreases below 340°C. The use of dissolved silica as a geo-thermometer has been derived from experimentally determined variations in the solubility of different silica species in water, as a function of temperature and pressure as well as from observations of well discharges and measured temperatures (Truesdell and Fournier, 1977; Fournier and Potter, 1982). The basic reaction for the solution of silica minerals to give dissolved silica is SiO_2 (s) + $_2H_2O$ = H_4SiO_4 (aq). The silica temperature is based on the equilibrium between quartz or chalcedony and the unionized silica in a thermal fluid. Experience shows that chalcedony temperature is commonly more realistic in low-temperature waters than quartz temperature (**Arnorsson 1975**). Both quartz and chalcedony geo-thermometers were used to estimate sub-surface temperatures. The following equations were used:

Quartz - no steam loss **(**Fournier, 1977)

$$T°C = (1309/(5.19-\log(SiO_2)))-273.15 \quad (1)$$

Chalcedony - no steam loss (Founier, 1977**)**

$$T°C = (1032/(4.69-\log(SiO_2)))-273.15 \quad (2)$$

Chalcedony - no steam loss, (Arnoórsson et al., 1983**)**

$$T°C = (1112/(4.91/\log(SiO_2)))-273.15 \quad (3)$$

5.5.2. Cation geo-thermometers

Cation geo-thermometers are also widely used to estimate sub-surface temperatures. The Na-K geo-thermometer is based on ion exchange reactions where in the equilibrium constants are dependent on temperature of partitioning of Na and K between hydrothermal altered aluminum silicates and solutions (Fournier and Truesdell, 1973). The ratio related to the general exchange reaction:

$$K^+ + \text{Na-feldspar} = \text{K-feldspar} + Na^+ \quad (4)$$

(Albite) (Orthoclase)

The equilibrium constant, *K,* for the Equation 4 is:

$$Keq = [KAlSiO_3O_8][Na^+]/[NaAlSi_3O_8][K^+] \quad (5)$$

If activities of the solid reactants are assumed to be in unity and the activity of dissolved species is almost equal to their molar concentrations, the equation will be reduced to: $Keq=[Na^+]/[K^+]$ (6)

Arnorsson et al., (1983**),** present the following formula based on empirical correlation; Giggenbach, (1981), Giggenbach, (1988) are used in this report; the concentrations of Na and K are in mg/kg:

Na/K temperature by Arnoórsson et al., (1983).

$$T°= (933/(0.993+\log(Na/K)))-273.15 \quad (7)$$

Na/K temperature by Giggenbach, (1988).

$$T°= (1390/(1.75+(Na/K)))-273.15 \quad (8)$$

The K-Mg geo-thermometer is based on the equilibrium between water and the mineral assemblage K-feldspar, K-mica and chlorite (Gigginbach, 1988). It is found that it responds quickly to changes in the physical environment and thus, usually gives a relatively low temperature in mixed and cooled waters as compared to other geo-thermometers (concentrations are in mg/kg).

$$T°= (4410/(14.0-\log (K^2/Mg^2))).-273.15 \quad (9)$$

Six equation geo-thermometers i.e. quart, chalcedony, Na-K and K-Mg were used in this study to estimate surface temperature of the reservoir. 6 equations belonging to these four equation geo-thermometers (Table 6).

5.6. Saturation Index

The computer program WATCH calculates the speciation of waters at a given temperature. It is useful for the interpretation of the chemical composition of geothermal fluids as well as for non-thermal waters. Chemical analysis of certain samples collected at the surface is used to compute the composition of aquifer fluids. The program calculates aqueous speculation using mass balance equations and chemical equilibrium. WATCH used to calculate the composition of the sample after cooling or boiling (Arnoórsson et al., 1983; Bjarnason, 1994), and is thus useful for modeling the behavior of water for different designs of the geothermal plant. Below are the three main conditions for geothermal fluids used into the computer program:

1) Two-phase inflow into well - in this case the discharge is also in two phases; hence, chemical data for both phases must be available. 2) Single-phase inflow into well - the discharge from the well can be either

single-phase or two-phase; this model also covers springs where the water is not boiled before collection. 3) Springs where the water is boiled and steam is lost before the samples collected.

The WATCH program can also be used to compute the concentrations of the resulting species, activity products and solubility products when the equilibrated fluid is allowed to cool conductivity or by adiabatic boiling from the reference temperature to some lower temperature. This is particularly useful in order to evaluate the scaling potential of the fluid. To evaluate the equilibrium minerals in the fluid, the WATCH program is run several times for all the wells from Kz 1 to Kz38; the chemical analysis is used for the water sample.

Table 6: The Result of the Geothermometers used

Well samples No.	K mg/l	Na mg/l	Mg mg/l	NaK/gig	NaK/ar	KMg /gig	Silica SiO_2 mg/l	T chalce	T quartz	T chal Ar
KZ1	2.0	36.6	34.8	186.846	138.813	21.659	13.800	17.544	50.050	21.801
KZ2	3.1	72.9	54.6	172.747	122.137	25.905	17.580	26.416	58.664	30.262
KZ3	4.7	112.2	49.6	171.141	120.259	34.109	21.800	34.768	66.714	38.200
KZ4	3.1	83.0	51.3	164.817	112.905	26.452	16.720	24.534	56.842	28.470
MD5	15.2	64.1	52.9	312.389	303.887	57.020	19.440	30.263	62.379	33.922
MD6	2.0	42.6	30.3	176.779	126.871	22.796	9.730	5.627	38.377	10.387
KZ7	7.1	121.0	66.0	192.958	146.150	39.212	11.100	10.003	42.677	14.584
KZ8	10.6	213.1	99.8	181.833	132.845	42.934	19.940	31.250	63.330	34.860
KZ9	2.3	51.8	31.3	174.861	124.616	25.386	19.000	29.379	61.526	33.081
KZ10	3.9	56.8	37.1	203.975	159.539	33.372	19.400	30.183	62.302	33.846
KZ11	8.2	245.0	133.0	157.881	104.916	35.346	11.200	10.306	42.974	14.875
KZ12	1.6	44.4	27.4	162.141	109.814	20.273	22.400	35.855	67.757	39.231
KZ13	1.6	41.4	29.2	166.323	114.650	19.734	18.300	27.940	60.137	31.712
KZ14	1.6	38.2	30.5	171.231	120.364	19.367	18.800	28.972	61.133	32.694
KZ15	8.2	238.7	79.6	159.328	106.575	40.210	19.700	30.779	62.876	34.412
KZ 16	7.8	102.6	54.6	211.330	168.600	42.911	16.600	24.266	56.582	28.214
KZ17	2.7	71.3	40.7	165.097	113.229	25.897	14.000	18.057	50.550	22.290
KZ18	3.1	86.7	58.4	161.679	109.281	25.152	15.100	20.781	53.201	24.892
KZ19	5.1	79.4	56.1	199.278	153.803	34.514	11.000	9.698	42.378	14.292
KZ20	2.0	37.5	30.8	184.992	136.600	22.655	9.530	4.949	37.709	9.736
KZ21	7.0	198.0	69.9	161.348	108.899	38.525	12.300	13.509	46.111	17.942
KZ22	7.0	174.0	79.4	169.106	117.885	37.311	11.200	10.306	42.974	14.875
KZ23	5.9	174.0	65.3	158.172	105.249	35.693	10.600	8.456	41.159	13.102
KZ24	7	148	69.3	178.858	129.324	38.499	15.100	20.781	53.201	24.892
KZ25	5.1	134	49.9	165.400	113.580	35.610	13.000	15.436	47.994	19.786
KZ26	5.5	170	78.1	155.851	102.592	32.847	13.900	17.801	50.301	22.046
KZ27	7	174.8	60.1	168.478	117.154	39.867				
KZ28	5.5	80.7		203.447	158.892		15.200	21.022	53.434	25.121
KZ29	7.4	153.2	62.4	180.205	130.916	40.579	20.200	31.756	63.817	35.341
KZ30	8.2	154.1	57.8	186.508	138.409	43.335	20.500	32.334	64.374	35.889
KZ32	5	41.2	25.2	248.245	215.606	41.772	11.600	11.497	44.142	16.016
KZ34	7	189.5	66.2	163.612	111.511	38.937	17.000	25.155	57.443	29.061
KZ35	8.6	186.8	70.3	177.143	127.300	42.347	14.200	18.564	51.044	22.775
Kz36	4.3	124.7	42.4	159.549	106.829	33.944	17.400	26.028	58.288	29.893
KZ37	7.8	206.5	69.3	164.945	113.053	40.583	17.700	26.673	58.913	30.507
KZ38	7.8	160.5	60.3	180.597	131.380	41.937	16.000	22.901	55.259	26.914

The (Figure 6**)** is composed of 14 graphs respectively representing well numbers Kz1, 2, 3, 4, MD5, 6, 7, 8, 18, 20, 21, 22, 30 and 36 that were selected on the basis of different locations, temperatures ,mineral equilibriums and structures. The graphs are constructed by the use of WATCH aqueous speciation program and they show log Q/K diagrams for the temperatures ranging from 20-120°C; this is useful to demonstrate reservoir temperatures. The diagrams show the saturation index log(Q/K) with the mixing equilibrium temperature for each mineral at log(QIK) = 0. The composition of graphs **(**Figure 6) represents the calculations performed using the WATCH aqueous speciation program to construct the mineral equilibrium diagrams. It shows the saturation index, log(Q/K) for temperature ranges from 20-120 °C for selected wells.

In the diagram, no best equilibrium temperatures can be found. This is probably due to mixing, and or other relevant processes such as the precipitation and leaching of some minerals.

As seen in the diagram, certain wells MD5, Kz30, Kz18, are close to equilibrium; chalcedony anhydrite and fluorite are at temperatures of approximately 100-115 °C for well MD5; re-equilibrated for well Kz30 for anhydrite, fluorite and epidote at temperature of 70-80 °C.

Much mixing at 115°C for well Kz18, close to equilibrium at 60 ^{0}C and higher mixing at 120 °C, and no equilibrium indicated for other graphs due to mixing with cold ground water.

Generally, the water is close to equilibrium with mineral calcite and quartz and under saturated with the minerals fluorite and anhydrite. For a few minerals equilibrium is indicated at 60-80^{0}C and mixing at higher temperatures up to 120 ^{0}C, which suggests mixing with cold groundwater. In addition, in well KZ30 there may

be re-equilibration of some minerals at a temperature of about 80 ^{0}C and mixing at higher temperature is indicated at about 115°C.

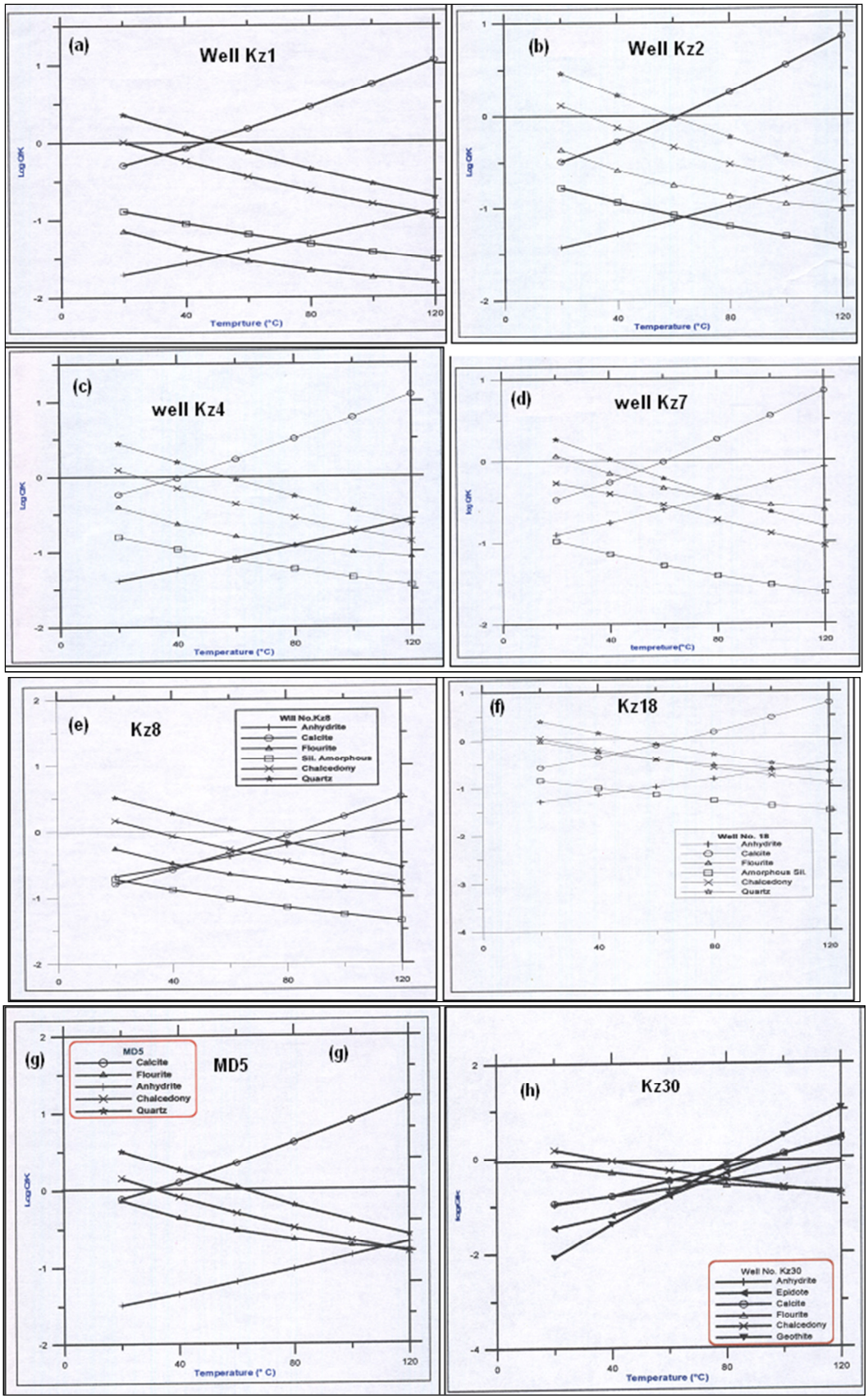

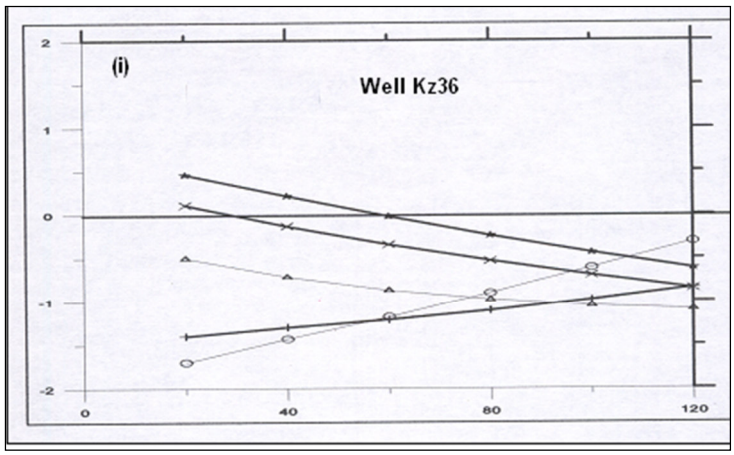

Figure 6. The graphs constructed by WATCH Program shows the saturation index Log(Q/K) with mixing equilibrium temperature for different minerals.

5.7. Mixing evaluations

5.7.1. Evidence of Mixing

Water formed by mixing geothermal water and cold groundwater or surface water may possess chemical characteristics which distinguish it from unmixed geothermal water. The reason is that the chemistry of geothermal water is characterized by equilibrium conditions between solutes and alteration minerals, whereas, the composition of cold water appears mostly to be determined by the kinetics of the leaching process. The residence time in the bedrock after mixing and the temperature and salinity of the mixed water have an influence on the final chemical composition in the spring discharge. Geothermal waters are often but not always much higher in dissolved solids than cold ground and surface waters. Strong conductive cooling of geothermal waters in up flow zones and subsequent reactions with the rock may produce compositional affinities similar to those obtained by leaching subsequent to mixing.

The main chemical characteristics of mixed waters, which distinguish them from equilibrated geothermal waters, include relatively high concentrations of silica in relation to the discharge temperature. Low pH relative to the water salinity and high total carbonate; at least if the mixing has prevented boiling and the temperature of the hot water component exceeds 200 ^{0}C. Mixed waters tend to be calcite under saturated and with low calcium/proton activity ratios compared with geothermal waters (Arnórsson, 1985).

The study of the thermal water from Khan Ezabeeb area shows strongly mixing of the water to the following reasons:

- There is a disagreement between different geo-thermometers;
- On the Giggenbach Na-K-Mg triangular diagram, all the samples fall in the partially equilibrated mixed water area.
- On the Giggenbach Cl-SO_4-HCO_3 diagram, most samples fall in the area of mixed waters.
- The mineral equilibria diagrams do not show clear crossing at zero saturation index by any group of minerals at the same temperature.
- There is a good agreement relationship between chloride versus ^{18}O, B and Br as suggested by Arnórsson, (1985).
- There is a similar trend for the cold and thermal waters plotted in the Schoeller diagram.

5.7.2. Mixing models

A plot of ^{18}O versus Chloride forms two distinct clusters - one of moderate geothermal water samples and another of well-mixed meteoric water samples representing well numbers Kz1, 6, 19 and 20, (Figure 7). The content of dissolved solids is appreciably higher in thermal wells than others due to chemical reactions between waters and rocks. The low chloride water relates local meteoric water, while high chloride relate to geothermal water samples (Tómasson, 1980). A linear relationship between Cl versus Br and B (Figure 8) is an indication of mixing (Arnorsson, 1985) except for a few scattered samples, which might be due to waters of different origin.

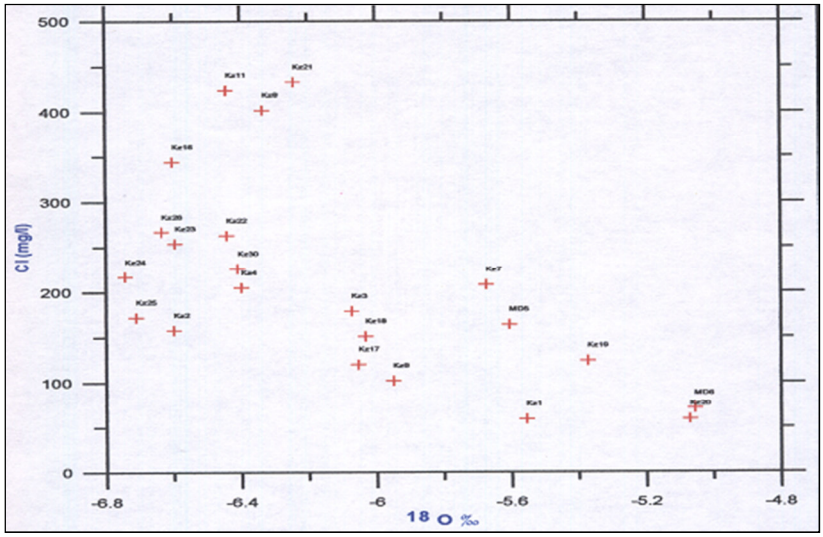

Figure 7: Mixing Models shows $\delta^{18}O$ versus Cl.

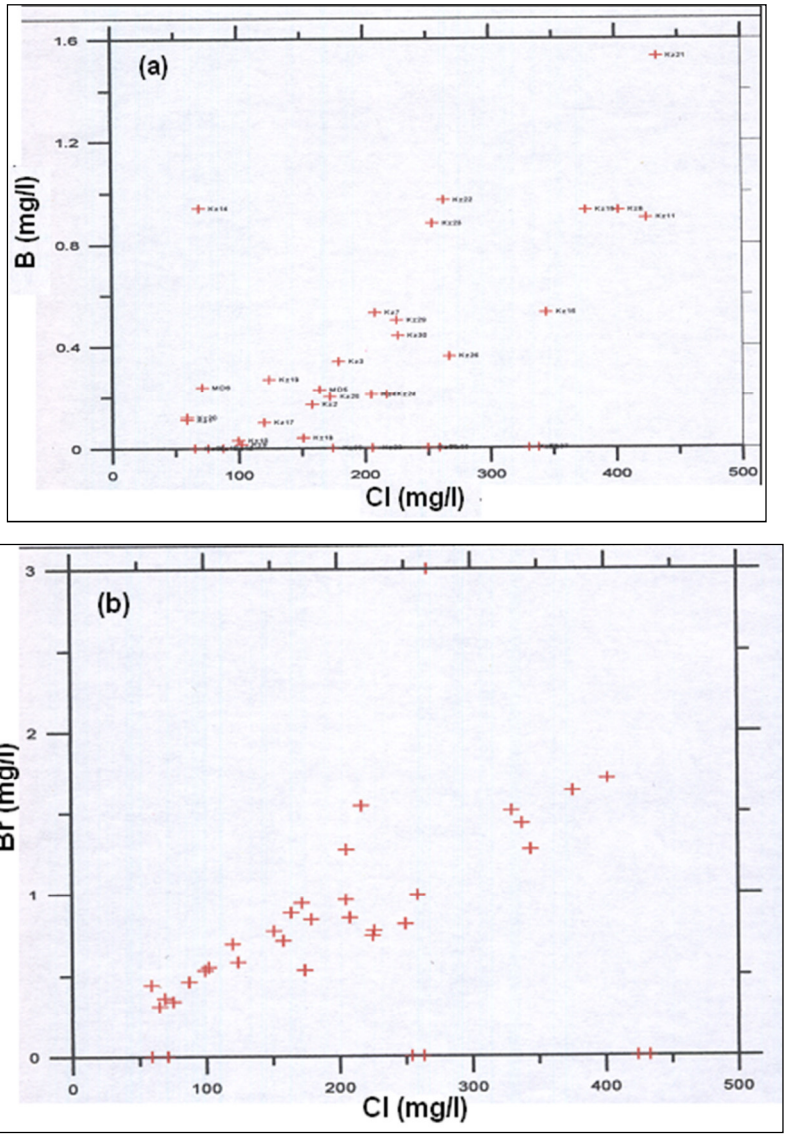

Figure 8: Mixing Models shows linear relationship between (a) Cl versus B and (b) Cl versus Br.

6. Discussion and Conclusions

The potential and geochemical properties of geothermal waters from the central Jordan (Khan Ezabeeb area) were studied to evaluate their possible use for desalinating the brackish water. The computer program WATCH calculated speciation in the waters and many different graphical representations were applied to give information about mineral equilibrium and estimates of the possible reservoir temperatures by the use of different geo-thermometers. Evaluation of mixing was made by use of different geochemical methods. Chemical analyses from 38 wells over a period of one year selected for interpretations - mainly well numbers Kz1, 2, 3, 4, 5, 6, 7, 8, 18, 20, 21, 22, 30 and 36. Certain wells selected on basis of high temperatures and mineral equilibrium - mainly well numbers Kz3, 5, 18, 22, 30 and 36. Seven wells Md5, Kz 9, 10, 22, 27, 30 and 31 selected for age determination purposes from all over the studied area depending on location and faults. The chemical composition of geothermal water indicates that no definite equilibrium temperatures can be appointed. The thermal fluids are rich in carbonate and the pH is less than 7, these result documented by Sawarieh, (2005) reported for the thermal water in shallow thermal wells in the resulted from mixing between the thermal chloride water of the lower aquifer with bicarbonate water of the upper aquifer.

Stable isotope interpretation data show no presence of any significant amount of magmatic water which generally has (^{18}O: +6 to +9‰ and ^{2}H: -40 to -80‰). The possibility of oceanic origin of these waters is ruled out because their (^{18}O and ^{2}H) are approximately 0‰. The origin of these waters is obviously meteoric. In $\delta^{18}O$ vs. δD diagram, the samples (except two outliers) make a trend line of equation: ($^{2}H = 5.7\ \delta^{18}O + 3.8$). The slope indicates dominance of evaporation/steam separation process. Location of all the data points below the LMWL (($^{2}H = 8\ (^{18}O + 25)$ also confirm evaporation process.

In a geothermal system, (^{34}S of sulphates with a magmatic origin ranges between 0‰ and +2‰ CDT (Canyon Diablo Troilite) and sulphates resulting from the dissolution of evaporates can have ^{34}S from +10 to +35‰, whereas in modern oceanic sulphates its value is about +20‰ (Krouse, 1980). The ^{34}S values of sulphates of hot springs are in the range of 6.56 to 10.81‰. It shows that the sulphates are neither of magmatic origin nor of modern oceanic origin. Relatively low values of ^{34}S indicate that the major contribution of sulphates derived from reduced sulphur compounds such as sulphide minerals and/or organic sulphides (Pearson et al., 1980).

The ^{14}C samples show that the age of the thermal fluids ranges between 20,000-37,000 years, the age from the fluid from well 31 is 20,000 year and well Kz22 and Kz27 is 30,000 years indicating an increasing age of the thermal water from North to South. This is in alignment with the other models, which suggest that the mixing of thermal fluids takes place in the Northern and Central parts of the field and a general flow direction is from North to South.

According to the mineral saturation index, none of the minerals is in equilibrium in Jordan; no definite mineral equilibrium temperature can be pin pointed. All the water samples study shows an evidence of considerable mixing, but there are indications for the existence of geothermal water up to about l00°C. the present studied by Gharaibeh, (2008**)** reported the heat sources of the thermal water in the lower aquifer is a result the deep circulation of water within the Paleozoic sandstone from slightly elevated geothermal gradient.

The temperature of the waters appears to be sufficiently high for special agricultural activities needing greenhouses or direct uses such as fish farming**),** and to grow flowers and mushrooms (Demange et. al., 1992**)**. Due to the bicarbonate water type, cares have been used in the design in order to prevent problems due to corrosion and scaling.

Acknowledgements

The authors are thankful to the General Director of Natural Resources Authority for support of the geothermal project. The authors are grateful to Engineer Drawish Jaser, coordinator of geothermal project and Geologist Mohammed Akour for support and co-operation. Special thanks to Engineer Suzan Kailani, head of isotopic section in the water authority, for help to chemical and isotope analysis, and Engineer Hasan for sharing his knowledge throughout the duration of the project. Authors are also thankful to, Mr. Esmail, the technician for his valuable time during sampling of the ^{14}C samples in the field.

REFERENCES

Arnórsson, S., (1975): Application of the silica geothermometer in low-temperature hydrothermal areas. in Iceland.; Am. J. of Sci., 275, 763-783.

Arnórsson, S., (1985): The use of mixing models and chemical geothermometers for estimating underground temperature in geothermal systems. J. Volc. Geotherm. Res., ,23**,** 299-335.

Arnórsson, S., (1991): Geochemistry and geothermal resources in Iceland, In: D'Amore,F. (co-ordinator), Applications ofgeochemistty in geot hermal reservoir development. UNITAR'UNDP publication, Rome, 145-196.145-196.

Arnórsson, S., Gunnlaugsson, E., and Svavarsson, H., (1983): The chemistry of geothermal waters in Iceland III.

Chemical geothermometry in geothermal investigations. Geochim. Cosmochim. Acta, 47, 567-577.
Bender, F., (1974): Geology of Jordan. Bortraeger, Berlin, , 196 pp.
Bjarnason, J.O., (1994): The speciation program WATCH, version 2.1. Orkustofhun, Reykjavik, 7pp.
Clark, I. D. and Fritz, P., (1998). Environmental Isotopes in Hydrogeology. Lewis Publishers, Boca Raton, New York.
Demange Gauthier, B., Martin, G., and Tournaye, D., (1992): Study for the use of geothermal resources for greenhouse heating, South Amman Zone, Kingdom of Jordan. Comp. Franc. Dc Geothermice, 141 pp.
DI Paola, G., (1981). Mission report on visit to the geothermal project JOR/76/004 in the Hashemite Kingdom of Jordan from 30 November to 4 December 1981. UN/DTCD Report, New York.
Fournier, R.O., (1977): Chemical geothermometers and mixing model for geothermal systems. Geothermics, 1977, 5, 41-50.
Fournier, R.O., and Potter, R.W. (1982): II: A revised and expanded silica (quartz) geothermometer. Geoth. Res. Council Bull., 11-10, 3-12.
Fournier, R.O., and Truesdell, A.H., (1973): An empirical Na-K-Ca geothermometer for natural waters.Geochim. Cosmochim. Acta, vol. 37, 1255-*1275.*
Futyan, A., (1968): Stratigraphy of Belqa 2 (.B2) and Belqa 3 (B3) of formations in Jordan and the origin of their bitumen**.** Natural Resources Authority, Amman, unpublished report.
Gharaibeh A., (2008): Heat Sources study and Geothermal Reservoir Assessment for the Zarqa Ma´in-Daba Area, Central Jordan. United Nations University, Geothermal Training Programme, Report Number 17. Pp.221-244.
Giggenbach, W. F., (1981):. Geothermal mineral equilibria. Geochim. Cosmochim. Acta, vol. 45, 393-410.
Giggenbach, W.F., (1988): Geothermal solute equilibria. Derivation of Na-K-Mg-Ca geoindicators. Geochim. Cosmochim. Acta,vol. 52**,** 2749-2765.
Giggenbach,W. F., (1991): Chemical techniques in geothermal exploration. In: D'Aniore,F. (coordinator), Application of geochemistry in geothermal reservoir development. UNITARIUNDP publication, Rome, 119-142.
Giggenbach, W. F.,(1992): Isotopic shift in waters from geothermal and volcanic systems along convergent plate boundaries ad their origin, Earth and Planetary Science Letters. 113: 495-510.
Jaser, D., (1986): The geology of Khan Ezabeeb, map sheet no.3253. Natural Resources Authority, geology directorate, Amman, Jordan.
Muffler P, Cataldi R. (1978): Methods for regional assessment of geothermal resources. Geothermics; 7: 53-89. doi:10.1016/0375-6505(78)90002-0
Nicholson, K. (1988): Geochemistry of geothermal fluids: An introduction. Geothermal Institute,
Saudi, A., (1999): The geochemistry of thermal fluids in the field near Alia airport in Jordan and Selfoss in Iceland, reports of the United Nations University.
Sawarieh, A., (2005): Hydrogeology of the Wadi Waleh sub-basin and Zarqa Main hot spring. University of London, UK, MSc. thesis, 60pp.
Tómasson, (1980): Selfoss geothermal area, S-Iceland. The using of chlorine as an indicator of an inflow of cold groundwater into the geothermal reservoir. Proceedings of 31 International Symposium on Water-Rock Interaction, Edmonton, Canada, July 107-109
Truesdell A.H., (1991): Effects of physical processes on geothermal fluids. In: D'Axnore,F. (coordinator), Application of geochemistry in geothermal reservoir development. UYIITAR/UNDP publication, Rome,vol. 7, 1-92.
Truesdell, A., (1979): Final report on the chemistry and geothermal energy possibilities of the Zara -Zarqa Ma'in springs, Jordan. U.S. Geol. Survey. Ment Park, , California.
Truesdell, A.H., and Fournier, R.O., (1977): Procedure for estimating the temperature of a hot water component in a mixed water using a plot of dissolved silica vs. enthalpy. US. Geol. SurveyJ. Res., vol. 5,49-52.
Krouse, HR., (1980): Sulphur isotopes in our environment, In: Fritz, P. and Fontes, J.-Ch., (Eds.) Handbook of Environmental Isotope Geochemistry, Vol. 1, Elsevier Scientific Publishing Company, Amsterdam-Oxford-New York: 227-257.
Pearson, F. J. and Hanshaw, B. B., (1970): Sources of Dissolved carbon species in groundwater and their effects on carbon-14 dating. In: Proceedings of IAEA Symposium on Isotope Hydrology. Vienna. 271-286.
Pearson, F.J.Jr. and Rightmire, C.T., (1980): Sulphur and oxygen isotopes in aqueous sulphur compounds, In: Fritz, P. and Fontes, LL-Ch., Handbook of Environmental Isotope Geochemistry, Vol.1. Elsevier Scientific Publishing Company, Amsterdam-Oxford-New
Pearson, F. J., (1965): Use of C-13/C-12 ratios to correct radiocarbon ages of material initially diluted by limestone. In: Proceedings of the 6th International of Radiocarbon and Tritium Dating. Pulman, Washington, June, USAEC Conf.-650652 (1965)357